

# **EVALUATION AND DEVELOPMENT OF SIMPLIFIED METHODS OF ANALYSIS OF THE INTEGRITY OF CRACKED REDUNDANT STRUCTURES**

C. Gallo, M. González-Posada, I. Gorrochategui and F. Gutiérrez-Solana

Departamento de Ciencia e Ingeniería del Terreno y de los Materiales  
Universidad de Cantabria. E.T.S.I de Caminos, C y P.  
Av. de los Castros s/n, 39005, Santander.

## **ABSTRACT**

This paper reviews and studies the various simplified procedures currently in use in the analysis of cracked sections. From the procedures evaluated, the most suitable one is selected and applied to the study of redundant structures.

The methods that analyse this type of cracked structures combine these simplified procedures with the Strength of Materials theory. For this, once the most suitable procedure has been selected, a comparison is made of the results obtained from the application of the Traditional Method of solving redundant structures with those obtained using the Variable Flexibility Method [1], the main difference between these methods being that the latter takes into account the redistribution of stresses in the structure when the cracks contained in it grow. The application of these two methods is illustrated through the resolution of an example of a cracked pipe.

## **1.- INTRODUCTION**

The necessity of evaluating the integrity of structures with the certainty of obtaining conservative conditions requires the analysis of industrial components to be as accurate as possible. One of the most common applications is the assessment of piping systems. These systems are usually hyperstatically supported and in some cases can contain defects in some of their sections.

The integrity of redundant cracked structures can be analysed by making combined use of simplified procedures of evaluation of cracked sections and the classic theory of Strength of Materials. The common way of combining these two procedures is known as 'Traditional Method'(TM). With this method the forces acting on the cracked section are calculated by the application of Strength of Materials theory, considering the component as uncracked. Then, the critical conditions of the cracked component are determined making use of the simplified procedures of evaluating cracked sections.

Another more realistic way to analyse this type of structures, is to take into account the change of the structural compliance and the redistribution of stresses when the flaw contained in the component propagates. The so-called 'Variable Flexibility Method' (VFM) evaluates the cracked structures in this way [1, 2]. This method also combines the theory of Strength of Materials with a simplified procedure, in this case GE-EPRI [3]. The main differences between the TM and VFM have already been reported in other works [1, 4].

After the publication of the VFM, new procedures for evaluating cracked sections have appeared (SINTAP) and some others have been improved (R6, ETM, ...). From the review and analysis of these existing simplified procedures, three of them have been selected to determine which one is the most appropriate for use in combination with Strength of Materials for structural assessment. This article reports a study where TM and VFM have been employed [5] to solve the same example and the results are compared and discussed.

## 2.- SELECTION OF SIMPLIFIED PROCEDURE

From the simplified procedures existing at this moment [6], three of them - GE-EPRI, Reference Stress and ETM - have been selected for the following reasons:

The GE-EPRI procedure was the first to be published and so it is a continuous reference for other procedures. It is also the one used in the VFM. The main drawbacks of this procedure are the limited number of  $J$ -integral solutions that are available in the bibliography and the necessity of fitting the material's behaviour to a Ramberg-Osgood law. This law is defined as:

$$\frac{\varepsilon}{\varepsilon_y} = \frac{\sigma}{\sigma_y} + \alpha \cdot \left( \frac{\sigma}{\sigma_y} \right)^n \quad (1)$$

where  $\sigma_y$  is the yield stress,  $\varepsilon_y$  is the corresponding strain  $\sigma_y/E$ ,  $n$  is the strain hardening coefficient and  $\alpha$  is a non-dimensional coefficient.

The Reference Stress procedure [7] is a simplification of the GE-EPRI procedure that substitutes the necessity of  $J$  solutions for the more commonly used  $K$  functions. This procedure has the advantage that it uses the real material's tensile behaviour.

The last one, ETM [8], has been recently updated. This procedure makes use of an approach similar to the GE-EPRI except that it obtains the  $J$ -integral applied to the cracked section from  $K$  solutions. These characteristics make this procedure more easily applicable than the other two: GE-EPRI and Reference Stress.

In this section, the results of evaluating the cracked sections using the three selected simplified procedures are included. Then, the results are compared to determine the most versatile procedure. This comparison is made by calculating with the different procedures the maximum bending moment that a tubular circumferentially through-wall cracked section (Figure 1) is able to bear.

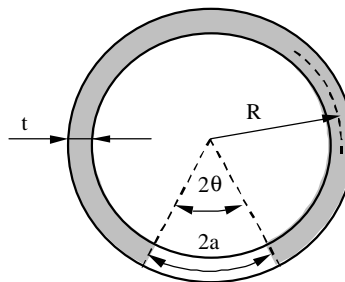


**Figure 1:** Cracked section

In order to perform the stability analysis of propagating flaws, the applied  $J$ -integral curve, as a function of the flaw size  $\theta/\pi$ , can be represented for parametric values of the applied bending moment  $M$  with the material's  $J_R$  curve. With this representation, it is possible to obtain the maximum bending moment that the cracked section can withstand as a function of the initial flaw size, considering that this section can also fail by the limit load criterion, named as  $M_{yy-cl}$ .

Figure 2 shows the results of the  $J$ -integral curves for different values of the applied bending moment, calculated with the three selected procedures compared with the material's  $J_R$  curve. It can be seen that all the procedures

lead to very similar estimations of the applied  $J$ -integral for the same values of the applied bending moment and flaw size.

The comparison between the maximum bending moments as a function of the initial flaw size, obtained by each procedure is presented in Figure 3. This figure indicates that, in general, the three procedures predict very similar estimations for any value of the initial flaw size. However, it can also be seen that the ETM and Reference Stress procedures present practically the same results, while the GE-EPRI differs a little. On the one hand, for bigger values of flaw size, this procedure is less conservative than the others because it predicts greater values of the bending moment sustained by the cracked section. On the other hand, for values of the initial flaw size lower than  $\theta_0/\pi = 0.1$ , it estimates lower values of this bending moment, being more conservative. This slight variation in the results is mainly due to the worse approximation of the material's tensile behaviour.

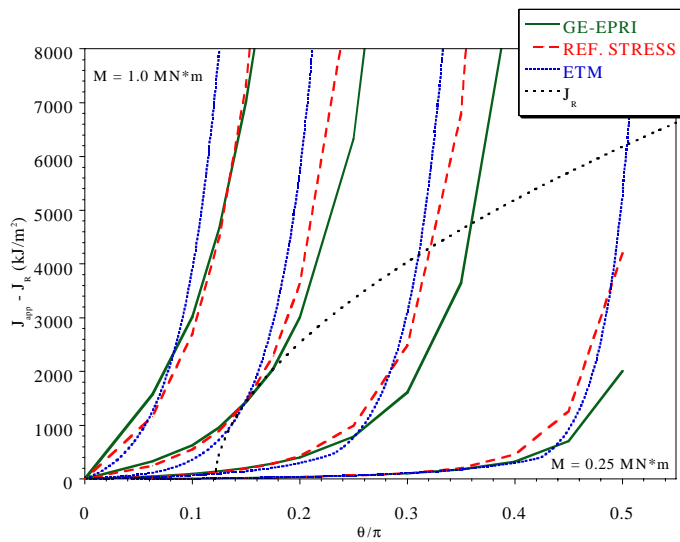


**Figure 2:**  $J$ -integral vs. crack size

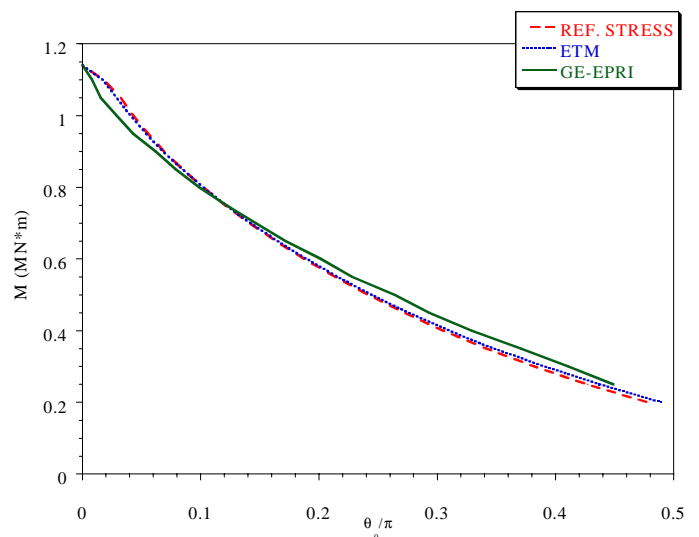


**Figure 3:** Maximum bending moment

The ETM procedure predicts conservative results in most of the studied situations. Also, this procedure makes a better approximation of the material's tensile behaviour, especially when the cracked section is near to the limit load. As in general the carbon steels, and in particular the material selected in this work, do not fit to the Ramberg-Osgood law and according to the considerations exposed in the beginning of this section about its simplicity, the ETM procedure has been selected to be combined with the Strength of Materials for the evaluation of cracked redundant structures in this work.

### 3.- HYPERSTATIC APPLICATION. COMPARISON BETWEEN METHODS.

The structural integrity of redundant cracked structures can be analysed either by the TM or by the VFM. As already mentioned, the main difference between these two methods is that the second one, the VFM, receives this name because it takes into account the variation in the flexibility of the elements that constitute the structure when the cracks they contain extend.

In this paper, the comparison between these two methods is carried out solving an example of a continuous pipe containing a circumferential through-wall flaw and obtaining the critical conditions of the structure for different values of the variables that influence it.

From this example, the areas of applicability of the different failure criteria of the cracked pipe are also defined on the basis of Fracture Mechanics. By comparing the results obtained by the two methods, it is possible to obtain conclusions on their applicability for evaluating hyperstatic cracked structures.

#### 3.1.- Description of the studied case

In this section the type of structure used for the application of the proposed methods of analysis and its

dimensions are described. Also, the characteristics of the postulated flaw in the structure are included defining its most significant dimensions.

The structure is the symmetrical continuous pipe of three spans represented in Figure 4. This pipe is simply supported and is subjected to two symmetrical vertical loads in its middle span. Furthermore, it contains a circumferential through-wall crack in the central section.

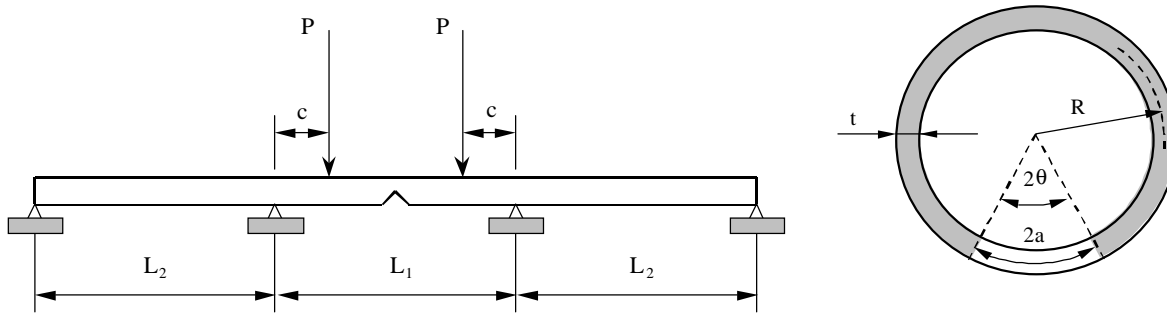


**Figure 4:** Studied case configuration

As the structural compliance influences the result of the highest load that the structure can bear, this effect has been considered solving the example for different values of the length of the external span  $L_2$ . The lengths selected are representative from the situation of a beam with fixed ends ( $L_2 = 0$ ), to the situation of a simply supported beam ( $L_2 = \infty$ ) and using 6, 12 and 24 m as intermediate values. The other geometric dimensions of the continuous pipe are  $L_1 = 6$  m and  $c = 1.5$  m.

The values that characterise the pipe transverse section are taken from a realistic element: 14 inches diameter, schedule 120. These values correspond to an external diameter  $D_0 = 355.6$  mm and a pipe thickness  $t = 27.8$  mm. The values considered for the size of the postulated flaw range from  $\theta/\pi = 0$  to  $\theta/\pi = 0.55$ .

The constituent material of the structure proposed in this example is a steel of very common use in current industrial installations: ASTM A 106 grade B [9]. The properties of this material have been obtained from a coupon taken from the piping system of an in-service power plant [10]. The most important mechanical properties of this material are included in TABLE 11.

**TABLE 1**

**MATERIAL MECHANICAL PROPERTIES**

| PROPERTY                         | SYMBOL     | VALUE                                   | UNITS                                   |
|----------------------------------|------------|---|---|
| <i>Yield Stress</i>              | $\sigma_y$ | 277.9                                   | MPa                                     |
| <i>Tensile Strength</i>          | $\sigma_u$ | 484                                     | MPa                                     |
| <i>Modulus of Elasticity</i>     | $E$        | 208500                                  | MPa                                     |
| <i>Ramberg-Osgood Parameters</i> | $n$        | 4.964                                   |   |
|                                  | $\alpha$   | 3.3031                                  |   |
| <i>ETM coefficient</i>           | $N$        | 0.1372                                  |   |
| <i>Toughness</i>                 | $J_R$      | $J_R = 309.4 \cdot (\Delta a)^{0.5678}$ | J in $\text{kJ/m}^2$ , $\Delta a$ in mm |

**3.2.- Failure criteria**

In this work, it has been considered that the analysed example can fail through three different mechanisms; these three failure criteria are:

- I. Unstable propagation in the cracked section: This criterion is reached when the forces acting on the cracked section are greater than the toughness of the material, causing the unstable extension of the defect. This mechanism is represented in the crack driving force diagrams (CDFD) when the applied  $J$ -integral curve is tangent to the material  $J_R$  curve (Figure 2). This criterion will be named as  $J_{app}$ .
- II. Limit load in the cracked section: This takes place when the obtained stresses in this section reach the flow stress of the material. This criterion will be named as  $M_{yy-cl}$ .
- III. Limit load in the sections located on the central supports: This takes place when the obtained stresses in these sections reach, in this case, the yield stress. The reason for choosing the yield stress as the limit stress in this criterion is in order to be consistent with the conventional assessment of uncracked structures. This criterion will be named as  $M_{y-ap}$ .

### 3.3.- Results

#### 3.3.1.- Traditional Method

The results obtained by the TM can be seen in Figure 5, expressed in terms of the value of the maximum load,  $P$ , as a function of the initial flaw size for different values of the external span length.

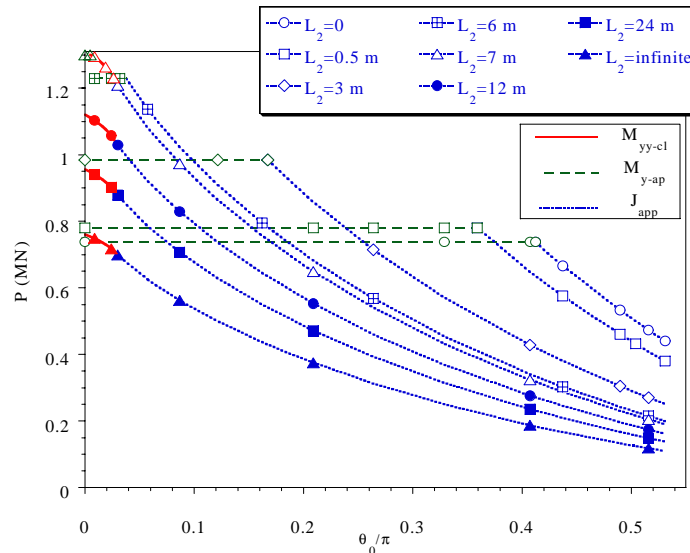


**Figure 5:** Maximum load calculated with the TM

It can be observed that the external span length  $L_2$  has a big influence on the maximum load borne by the cracked structure. This influence is variable depending on the prevailing failure mechanism. For example, for a value of initial flaw size  $\theta_0/\pi = 0.5$ , where the unstable propagation criterion (I) prevails, the maximum load borne by the cracked structure is higher for lower lengths of the external span.

For medium values of the initial flaw size, two different failure mechanisms can occur depending on  $L_2$ . For example, for  $\theta_0/\pi = 0.15$  and  $L_2 \leq 3$  m, the structure is limited by the yielding load of the sections located on the central supports (III); however, for  $L_2 > 3$  m, the dominating failure criterion is again criterion I.

Finally, for small initial flaw sizes, some of the limit load criteria (II or III) are always applicable. The acting one depends again on  $L_2$ , criterion III when  $L_2 \leq 6$  m and criterion II when  $L_2 > 6$  m. In this range, the dependency of the maximum load with respect to the external span length is different for the two acting failure mechanisms.

#### 3.3.2.- Variable Flexibility Method

A typical representation of a crack driving force diagram (CDFD) in terms of the applied  $J$ -integral vs. crack length for different values of applied load is shown in Figure 6. In this figure the material  $J_R$  curve and the two limit load criteria are also shown. It can be observed that the  $J_R$  curve can be tangent to the applied  $J$ -integral

curves depending on the initial flaw size, as for example the one represented in this figure corresponding to a load  $P = 0.975$  MN. In this case, the unstable propagation criterion prevails. When these curves do not achieve the tangency condition inside the applicable range, one of the other two criteria prevail and the limit load is identified by the point where the  $J_R$  curve intersects the curves represented either as  $M_{yy-cl}$  or  $M_{y-ap}$ .

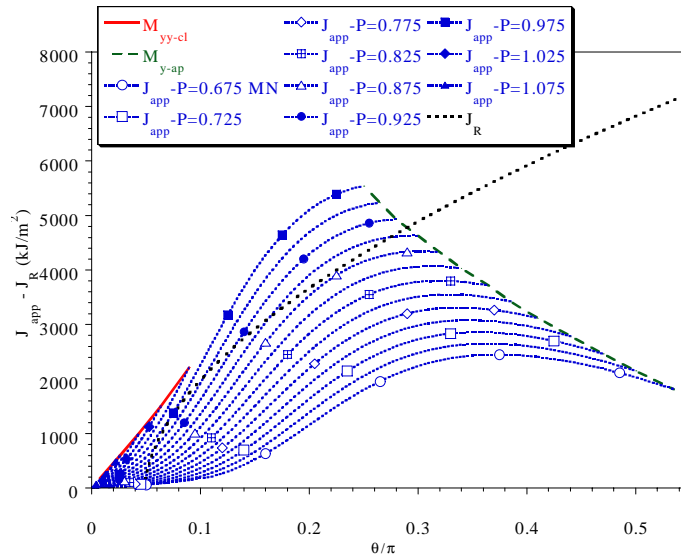


**Figure 6:** VFM crack driving force diagram

The results obtained with the VFM are represented in Figure 7. The result presented is the maximum load allowed by the cracked structure as a function of the initial flaw size for different values of the external span length.

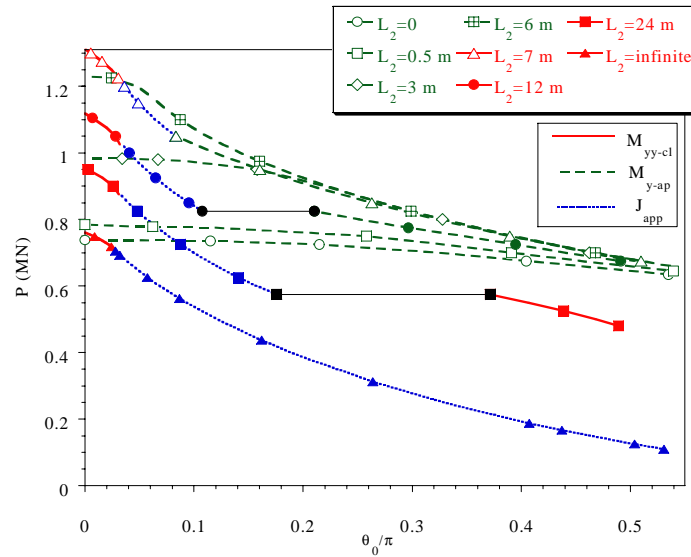


**Figure 7:** Maximum load calculated with the VFM

In this figure, the existence of a horizontal portion in the curves of lengths 12 and 24 m can be observed. The cause of this behaviour is that the failure mechanism considered as criterion I is the first occurrence of unstable crack propagation and the possibility of crack arrest has not been taken into account.

As expected, it can also be seen in this figure that the value of maximum load borne by the cracked structure,  $P$ , is lower when the value of initial flaw size increases. This trend is more or less pronounced depending on  $L_2$ . For example, when  $L_2 = 0.5$  m,  $P$  has only a little variation between the initial flaw size zero and the value  $\theta/\pi = 0.5$ . However, the difference in these values for  $L_2 = 7$  m is more pronounced.

On the one hand, for the same value of flaw size, it can be seen that the maximum load carried by the cracked structure increases when the value of external length grows if the acting failure mechanism is criterion III. For example, for  $\theta/\pi = 0.02$ , the value of  $P$  increases from 0.75 MN when  $L_2 = 0$  to 1.25 MN when  $L_2 = 7$  m. On

the other hand, this behaviour is reversed when the failure occurs in the middle section of the beam, either by plastic collapse or unstable propagation.

### 3.4.- Discussion

To evaluate the differences between the two methods, the results obtained by each method are compared in Figures 8 and 9. These figures show the maximum load carried by the cracked structure as a function of the initial flaw size for different values of the external span length.

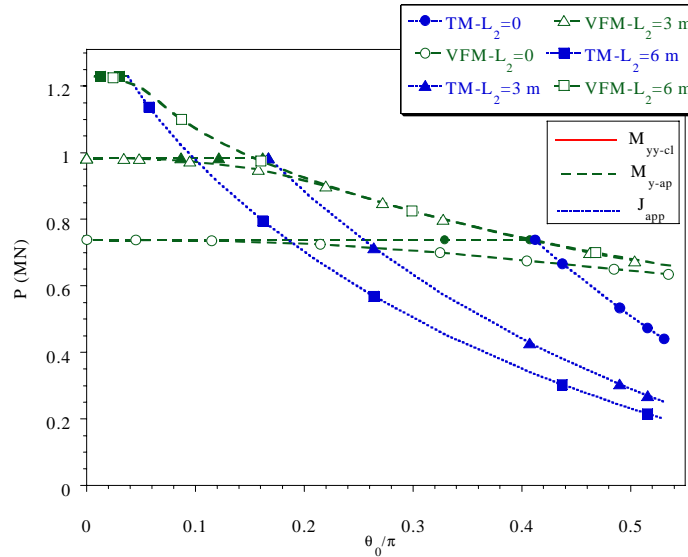


**Figure 8:** Comparison of results for low values of  $L_2$

Figure 8 shows the curves for  $L_2 = 0, 3,$  and  $6$  m. Taking the results obtained by the VFM as the reference, it can be observed that for small initial flaw sizes the TM predicts slightly higher values of the maximum load, being these differences more pronounced when the value of initial flaw size increases. This consideration only applies when the acting failure criterion predicted by both methods is criterion III,  $M_{y-ap}$ . However, in general, VFM is the method that predicts higher estimations of the maximum load, up to a factor of three. This is because the failure mechanism predicted by both methods is different, being criterion I for the VFM and criterion III for the TM. In conclusion, the TM is conservative but defining a different failure criterion, except for a limited range of flaw sizes where it can be slightly non-conservative.

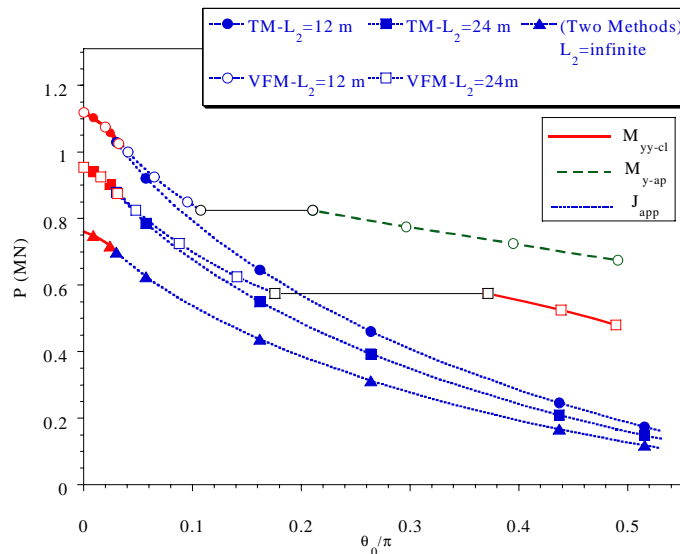


**Figure 9:** Comparison of results for high values of  $L_2$

Figure 9 shows the same curves of maximum load obtained for external span lengths  $L_2 = 12, 24$  m and infinite.

It can be seen that for small initial flaw sizes, where the failure criteria are the same, the predictions of the maximum load carried by the structure are similar, the TM results being a little more conservative. However, for high flaw size values, the criteria of failure are different and the predictions of each method separate. The TM results are in this case over conservative, up to a factor of four, compared to those of the VFM.

#### 4.- CONCLUSIONS

A revision has been made of the existing simplified procedures of evaluating cracked sections and three of them have been selected for comparative purposes. The different procedures use different approximations of the stress-strain curve of the material and a different approach to calculate the applied  $J$ -integral. As the three procedures lead to similar estimations of the section loading capacity, the most versatile one, the ETM, has been chosen to be used in combination with the Strength of Materials theory in the calculations carried out in this work.

Through the resolution of a realistic example of a hyperstatic structure, the different failure mechanisms have been precisely defined: unstable propagation or plastic collapse of the mid-section and plastic collapse of the section located on the central supports. The range of applicability of each one depends on the loading, the flaw size and the geometrical configuration of the analysed beam.

The final and most important conclusion is that the TM is always conservative except when simultaneously the initial flaw size and the external span length are low. In this case, the estimations obtained by this method are only slightly unsafe. On the other hand, the predictions obtained by the TM tend to be too conservative for high values of the initial flaw size. The reason for this difference is the different failure criteria predicted by the two methods.

#### 5.- REFERENCES

1. Gorrochategui, I. (1993). Comportamiento en Rotura de Tuberías de Alta Tenacidad con Sustentación Hiperestática en Régimen Elastoplástico. Tesis Doctoral, E.T.S. de Ingenieros de Caminos, Canales y Puertos, Universidad de Cantabria.
2. Gorrochategui, I., Gutiérrez-Solana, F. (1998). A Method for the Assessment of Hyperstatic Cracked Structures in the Elastic-Plastic Regime. *Engineering Fracture Mechanics* 61, pp.519-535.
3. Kumar, V., German, M. D. and Shih, C. F., (1981). "An Engineering Approach for Elastic-Plastic Fracture Analysis", General Electric Company, NP-1931, Research Project 1237-1, Topical Report, Schenectady, New York.
4. Gorrochategui, I., Gutiérrez-Solana, F., Ruiz, J. (1998). Parametric Study of the Failure of Statically Indeterminate Cracked Pipes. In: Edwards J. H., Flewitt P. E., Gasper B. C., McLarty K. A., Stanley P., Tomkins B. editors. EMAS Publishing, West Midlands UK. Lifetime Management and Evaluation of Plants, Structures and Components. Proceedings of the 4th International Conference of Engineering Structural Integrity Assessment.
5. Gallo, C. (1999). Evaluación y Desarrollo de Métodos Simplificados de Análisis de Estructuras Hiperestáticas Agrietadas en Régimen Elastoplástico. Proyecto Fin de Carrera. , E.T.S. de Ingenieros de Caminos, Canales y Puertos, Universidad de Cantabria.
6. Ruiz, J., González-Posada, M. A., Gorrochategui, I., Gutiérrez-Solana, F. (1998), Análisis Comparativo de los Procedimientos de Evaluación de la Integridad Estructural de Componentes Fisurados, *Anales de Mecánica de la Fractura*, Vol. 15, pp.115-119.
7. Anderson, T. L. (1991). "Fracture Mechanics, Fundamentals and Applications", Department of Mechanical Engineering Texas A&M University, College Station Texas.
8. Schwalbe, K.-H., Zerbst, U., Kim, Y.-J., Brocks, W., Cornec, A., Heerens, J., Amstutz, H., (1998). "EFAM ETM 97", GKSS-Forschungszentrum Geesthacht GmbH.-Geesthacht
9. ASTM A 106- "Standard Specification for Seamless Carbon Steel Pipe for High-Temperature Service", American Society for Testing and Materials.
10. Departamento de Ciencia e Ingeniería del Terreno y de los Materiales, Universidad de Cantabria. (1999). Tenacidad de aceros Estructurales de Sistemas Nucleares (Caracterización del Material). Internal report.